

Displacement and annihilation of Dirac gap-nodes in d -wave iron-based superconductors

Andrey V. Chubukov,¹ Oskar Vafek,² and Rafael M. Fernandes¹

¹*School of Physics and Astronomy, University of Minnesota, Minneapolis, MN 55455, USA*

²*Department of Physics and National High Magnetic Field Laboratory, Florida State University, Tallahassee, Florida 32306 USA*

(Dated: December 9, 2024)

Several experimental and theoretical arguments have been made in favor of a d -wave symmetry for the superconducting state in some Fe-based materials. It is a common belief that a d -wave gap in the Fe-based superconductors must have nodes on the Fermi surfaces centered at the Γ point of the Brillouin zone. Here we show that while this is the case for a single Fermi surface made out of a single orbital, the situation is more complex if there is an even number of Fermi surfaces made out of different orbitals. In particular, we show that for the two Γ -centered hole Fermi surfaces made out of d_{xz} and d_{yz} orbitals, the d -wave gaps have no nodes on each of the Fermi surfaces. The nodal points still exist near T_c along the symmetry-imposed directions, but are displaced to momenta between the two Fermi surfaces. At a smaller temperature, these nodal points can merge and annihilate, making the d -wave state completely nodeless. These results imply that photoemission evidence for a nodeless gap on the d_{xz}/d_{yz} Fermi surfaces of KFe_2As_2 does not rule out d -wave gap symmetry in this material, while a nodeless gap observed on the d_{xy} pocket in $\text{K}_x\text{Fe}_{2-y}\text{Se}_2$ is inconsistent with the d -wave gap symmetry.

PACS numbers: 74.20.Rp, 74.25.Nf, 74.62.Dh

I. INTRODUCTION

One of the most interesting features of Fe-based superconductors (FeSC) is the observation of different structures of the superconducting (SC) gap in different materials, which may indicate that the gap symmetry in FeSC is material dependent.¹ Weakly or moderately doped FeSC have both hole and electron pockets, and the gap symmetry there is very likely s -wave, with a π phase shift between hole pockets and electron pockets – the so-called s^{+-} -wave state². The situation is less clear in materials with only one type of Fermi pocket, such as strongly hole doped KFe_2As_2 , which contain only hole pockets³, and $\text{K}_x\text{Fe}_{2-y}\text{Se}_2$ or monolayer FeSe, which have only electron pockets⁵. Thermal conductivity and Raman scattering measurements in KFe_2As_2 ^{6,7}, as well as the observation of a neutron resonance peak in the superconducting state of $\text{K}_x\text{Fe}_{2-y}\text{Se}_2$ ⁸, were interpreted as evidence for a d -wave gap symmetry in these materials. Theoretical studies also found a strong enhancement of the d -wave superconducting susceptibility^{10,12}, and at least one study of KFe_2As_2 have found¹¹ a much stronger attraction in the d -wave channel than in the s^{+-} channel.

The arguments in favor of a d -wave gap symmetry, however, have been questioned by angle-resolved photoemission (ARPES) measurements^{4,13}. For hole-doped KFe_2As_2 , these measurements have found¹³ that the gap on the inner hole pocket centered at the Γ point ($\mathbf{k} = 0$) displays some angle variation but has no nodes¹⁴. The conventional wisdom is that a d -wave gap must vanish along symmetry-imposed directions in momentum space on all Fermi surfaces centered at $\mathbf{k} = 0$ – specifically, along the diagonals $k_x = \pm k_y$ in the 1-Fe Brillouin zone when the gap has $d_{x^2-y^2}$ symmetry, which is

the case considered hereafter. The non-vanishing of the gap along these direction in ARPES measurements was interpreted¹³ as the smoking-gun evidence ruling out a d -wave gap in KFe_2As_2 . Similarly, in $\text{K}_x\text{Fe}_{2-y}\text{Se}_2$, the gap has been measured on the electron pocket centered at the Z -point ($k_x = k_y = 0$ and $k_z = \pi$), and was found to be almost angle-independent⁹. Again, the conventional wisdom is that this result is fundamentally inconsistent with a d -wave gap symmetry.

In this paper we argue that the structure of the d -wave gap along the Fermi surfaces (FS) of FeSC, which are multi-orbital/multi-band superconductors, can be qualitatively different from the case of a single-band d -wave superconductor. Specifically, we show that, while the d -wave gap has symmetry-imposed nodes on a single-orbital pocket centered at $k_x = k_y = 0$, it has no nodes on pockets made out of different orbitals. In particular, we demonstrate that the d -wave gap *does not have nodes* on the two Γ -centered hole pockets made out of d_{xz}/d_{yz} orbitals, as shown in Fig. 1a. This behavior is ultimately related to how intra-orbital pairing in the orbital basis is displayed in the band basis¹⁵. In particular, in the absence of spin-orbit interaction, tetragonal symmetry requires that the d -wave gap on these pockets must be diagonal in the orbital basis, i.e. $\langle d_{xz,-\mathbf{k}\downarrow}d_{xz,\mathbf{k}\uparrow} \rangle = \Delta$, $\langle d_{yz,-\mathbf{k}\downarrow}d_{yz,\mathbf{k}\uparrow} \rangle = -\Delta$. However, to analyze the gap structure near the FS, one needs to change basis from orbital space to band space, characterized by the band operators $c_{1,\mathbf{k}\sigma}$ and $c_{2,\mathbf{k}\sigma}$, which describe excitations near the two hole FS. As a result, in band basis, the same d -wave gap acquires both diagonal and off-diagonal components: $\langle c_{1,-\mathbf{k}\downarrow}c_{1,\mathbf{k}\uparrow} \rangle = -\langle c_{2,-\mathbf{k}\downarrow}c_{2,\mathbf{k}\uparrow} \rangle = \Delta \cos 2\theta$ and $\langle c_{2,-\mathbf{k}\downarrow}c_{1,\mathbf{k}\uparrow} \rangle = \langle c_{1,-\mathbf{k}\downarrow}c_{2,\mathbf{k}\uparrow} \rangle = \Delta \sin 2\theta$, respectively. For circular and small hole FS, θ coincides with the angle

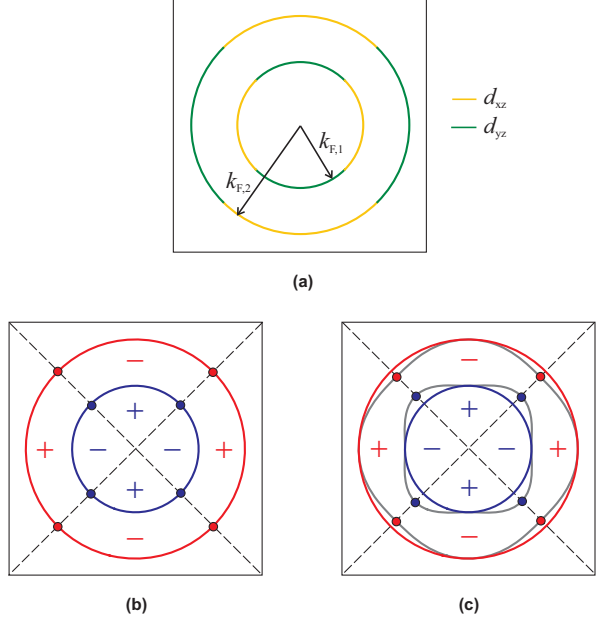


FIG. 1: The Fermi surfaces (FS) and the location of the nodal points near the two Γ -centered d_{xz}/d_{yz} pockets. Panel (a) shows the two FS in the normal state, highlighting the orbital that gives the largest spectral weight at each point along the FS (yellow for d_{xz} and green for d_{yz}). Panel (b) illustrates the location of the d -wave nodes on the two FS (blue and red lines) if the band off-diagonal gap term was absent. Panel (c) presents the actual location of the nodal points (red and blue dots) for the case $\Delta = 0.8\Delta_{\text{cr}}$. The dispersions are given by $E_{a,b} = \sqrt{\Delta^2 \cos^2 2\theta + \epsilon_{a,b}^2}$ and the terms $\epsilon_{a,b}$ vanish along the two gray lines adjacent to the FS.

along the FS.

Because the off-diagonal gap term mixes the two FS, the d -wave gap varies as function of θ but does not have nodes. The strength of the mixing depends on the interplay between Δ and the splitting between the two hole FS, as we discuss below. Such an effect does not happen for an s -wave gap, since the orbital and band representations are identical in this case, implying that off-diagonal terms do not emerge. In this situation, accidental nodes on any FS are possible. The orbital and the band representations are also identical, for any gap symmetry, on a pocket made out of a single orbital, such as the d_{xy} Z -pocket in $\text{K}_x\text{Fe}_{2-y}\text{Se}_2$.

Our analysis reveals that the nodes in the d -wave excitation spectrum near the d_{xz}/d_{yz} hole pockets do survive, at least near T_c , but displaced from the two hole FS. In particular, the excitation spectrum acquires the form

$$E_{a,b}^2 = \Delta^2 \cos^2 2\theta + \epsilon_{a,b}^2 \quad (1)$$

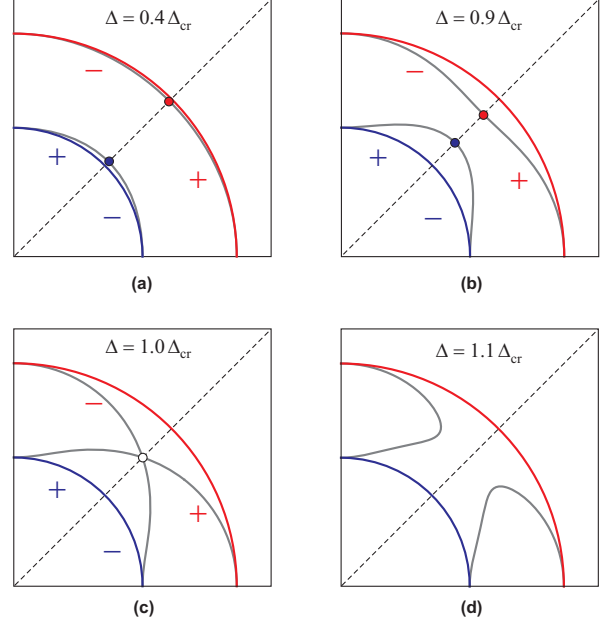


FIG. 2: The evolution of the d -wave nodes as Δ increases beyond the critical value Δ_{cr} . The blue and red lines are the normal state FS. The gray lines denote the locations of $\epsilon_{a,b} = 0$, and the dispersions are given by $E_{a,b} = \sqrt{\Delta^2 \cos^2 2\theta + \epsilon_{a,b}^2}$. The nodal points are marked by the red and blue dots. Four pairs of nodal points are present for $\Delta < \Delta_{\text{cr}}$ and disappear for $\Delta > \Delta_{\text{cr}}$. In this figure, we used circular band dispersions with $m_2 = 3m_1$.

with

$$\epsilon_{a,b} = \text{sgn}(\epsilon_{1,\mathbf{k}} + \epsilon_{2,\mathbf{k}}) \sqrt{\left(\frac{\epsilon_{1,\mathbf{k}} + \epsilon_{2,\mathbf{k}}}{2}\right)^2 + \Delta^2 \sin^2 2\theta} \pm \left(\frac{\epsilon_{1,\mathbf{k}} - \epsilon_{2,\mathbf{k}}}{2}\right) \quad (2)$$

where $\epsilon_{1,\mathbf{k}}$ and $\epsilon_{2,\mathbf{k}}$ are the normal state dispersions of bands 1 and 2, respectively. If the off-diagonal term $\Delta \sin 2\theta$ was absent, $\epsilon_a = \epsilon_{1,\mathbf{k}}$, $\epsilon_b = \epsilon_{2,\mathbf{k}}$, and the dispersions would be the conventional ones for a d -wave SC, namely, $E_{a,b}^2 = \Delta^2 \cos^2 2\theta + \epsilon_{1,2}^2$. In this case, each dispersion would have nodal points on the FS at $\theta = \theta_n \equiv (2n+1)\pi/4$, with $n = 0, 1, 2, 3$ (see Fig. 1b). Because of the off-diagonal term, however, ϵ_a does not vanish when $\epsilon_1 = 0$ and ϵ_b does not vanish when $\epsilon_2 = 0$. However ϵ_a (ϵ_b) does vanish along the lines specified by $\epsilon_{1,\mathbf{k}}\epsilon_{2,\mathbf{k}} = -\Delta^2 \sin^2 2\theta$, which are displaced from the actual FS, see Fig. 1c.

When the magnitude of the d -wave gap is small, the two lines are well separated and cross the direction $\theta = \theta_n$ at the momenta $k_a > k_{F,1}$ and $k_b < k_{F,2}$. At these crossing points, the full quasiparticle energy E_a (E_b) vanishes. These are new d -wave nodal points, shifted from their corresponding FS by the mixing term. For small Δ , this shift is small, of order Δ^2 . However, as temperature decreases, Δ becomes larger and the nodal points become

closer. If the gap reaches the critical value Δ_{cr} , which depends on the radii of the two pockets, the two nodal points merge and annihilate each other. In particular, at the Lifshitz transition taking place for $\Delta = \Delta_{\text{cr}}$, the $\epsilon_a = 0$ and $\epsilon_b = 0$ lines mix and split in the orthogonal direction, see Fig. 2. For $\Delta > \Delta_{\text{cr}}$, these lines no longer cross the directions $\theta = \theta_n$, i.e. $\epsilon_{a,b}$ and $\Delta \cos 2\theta$ do not vanish simultaneously. In this situation, $E_{a,b}$ do not have nodal points, implying that the excitations of the d -wave superconductor are fully gapped.

When nodal points are present, the excitations near $E_{a,b} = 0$ are Dirac-cones, $E_{a,b} = \sqrt{\tilde{k}_x^2 + \tilde{k}_y^2}$, where \tilde{x} and \tilde{y} are directions along and transverse to the lines $\epsilon_a = \epsilon_b = 0$, defined by $k_x = 2\Delta(\theta - \theta_n)$ and $\tilde{k}_y = (\frac{d\epsilon_{a,b}}{dk})(k - k_{a,b})$, where the derivative is taken at $\theta = \theta_n$. At the critical gap value $\Delta = \Delta_{\text{cr}}$, because $d\epsilon_{a,b}/dk$ vanishes we find $\tilde{k}_y \propto (k - k_{a,b})^2$. This dispersion has the same form as the dispersion of fermions at the critical point between a semi-metal and an insulator^{18–20}. It was argued¹⁹ that for such a dispersion the system with dynamically screened Coulomb interaction should display a highly non-trivial quantum-critical behavior in both fermionic and bosonic sectors. Our study shows that a d -wave FeSC provides an interesting realization of such a behavior.

The structure of the d -wave gap in multi-orbital FeSCs has been recently analyzed in²¹. That work focused on the gap on the electron pockets. We, on the contrary, analyze the gap structure on the two Γ -centered d_{xz}/d_{yz} hole pockets, where the inter-pocket gap component, induced by the orbital composition of the pockets, plays a crucial role.

The paper is organized as follows: in Section II, we introduce the model, in Section III we derive the excitation spectrum, in Section IV we compare our results with the case of a semi-metal to insulator transition, and in Section V we present our conclusions.

II. MODEL FOR d -WAVE SUPERCONDUCTIVITY

To focus on the main message of this paper, we consider a simplified model of an FeSC with two Γ -centered hole pockets made out of the d_{xz} and d_{yz} orbitals (Fig. 1a), and assume that 4-fermion interactions give rise to d -wave superconductivity with $d_{x^2-y^2}$ gap symmetry (for a d_{xy} gap symmetry, the results are analogous to the ones that we obtain below). The attraction in the d -wave channel may be due to the interactions within the d_{xz}/d_{yz} subset, as we assume for simplicity, or it can be induced by the coupling to other orbitals. In the $d_{x^2-y^2}$ ordered state, which belongs to the B_{1g} irreducible representation of the D_{4h} group, the gap function in the orbital basis is given by $\langle d_{xz,-\mathbf{k}\downarrow} d_{xz,\mathbf{k}\uparrow} \rangle = \Delta$, $\langle d_{yz,-\mathbf{k}\downarrow} d_{yz,\mathbf{k}\uparrow} \rangle = -\Delta$. There are no inter-orbital terms $\langle d_{yz,-\mathbf{k}\downarrow} d_{xz,\mathbf{k}\uparrow} \pm d_{xz,-\mathbf{k}\downarrow} d_{yz,\mathbf{k}\uparrow} \rangle$ as they belong to

the different irreducible representations B_{2g} (plus sign) and A_{2g} (minus sign).

Although the anomalous terms $\langle d_{i,-\mathbf{k}\downarrow} d_{j,\mathbf{k}\uparrow} \rangle$ are diagonal, the kinetic energy near the Γ point does contain terms describing hopping from one orbital to the other. The kinetic energy is diagonalized by converting from the orbital to the band basis, yielding:

$$\mathcal{H}_0 = \sum_{\mathbf{k},\alpha} \left(\epsilon_{1,\mathbf{k}} c_{1,\mathbf{k}\alpha}^\dagger c_{1,\mathbf{k}\alpha} + \epsilon_{2,\mathbf{k}} c_{2,\mathbf{k}\alpha}^\dagger c_{2,\mathbf{k}\alpha} \right). \quad (3)$$

The dispersions $\epsilon_{1,k}$ and $\epsilon_{2,k}$ are C_4 -symmetric. We assume for simplicity that the system parameters are such that the hole pockets can be approximated as circular¹⁶, i.e. $\epsilon_{1,\mathbf{k}} = \mu - k^2/(2m_1)$ and $\epsilon_{2,\mathbf{k}} = \mu - k^2/(2m_2)$. The two dispersions are not identical when $m_1 \neq m_2$, but are degenerate by symmetry at $\mathbf{k} = 0$ in the absence of spin-orbit coupling^{22,23}.

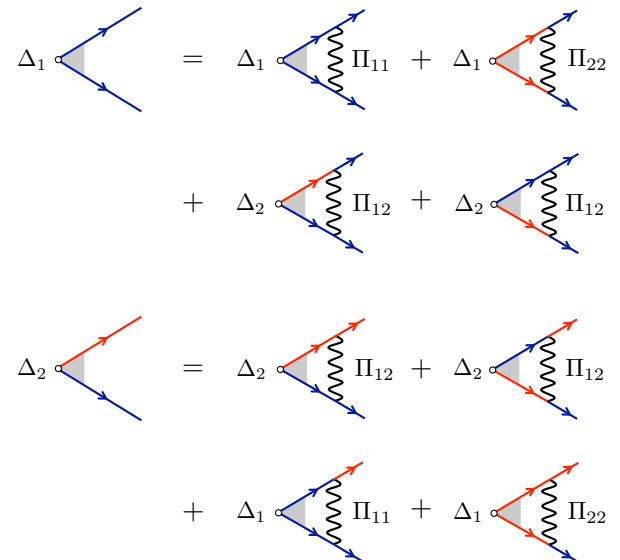


FIG. 3: The diagrammatic representation of the linearized gap equations, Eqs. 8. Blue and red lines denote fermions from bands c_1 and c_2 .

The transformation from the orbital operators d_{xz}/d_{yz} to the band operators c_1 and c_2 is a $U(1)$ rotation:

$$\begin{aligned} d_{xz,\mathbf{k}\alpha} &= \cos \theta_{\mathbf{k}} c_{1,\mathbf{k}\alpha} + \sin \theta_{\mathbf{k}} c_{2,\mathbf{k}\alpha}, \\ d_{yz,\mathbf{k}\alpha} &= \cos \theta_{\mathbf{k}} c_{2,\mathbf{k}\alpha} - \sin \theta_{\mathbf{k}} c_{1,\mathbf{k}\alpha}, \end{aligned} \quad (4)$$

For circular Fermi pockets the rotation angle $\theta_{\mathbf{k}}$ coincides with the polar angle θ along the FS¹⁶. Using Eq. (4) we also re-express the anomalous term $\mathcal{H}_\Delta = \Delta \sum_{\mathbf{k}} (d_{xz,\mathbf{k}\uparrow}^\dagger d_{xz,-\mathbf{k}\downarrow}^\dagger - d_{yz,\mathbf{k}\uparrow}^\dagger d_{yz,-\mathbf{k}\downarrow}^\dagger)$ in the band basis. We obtain a combination of inter-band and intra-band terms:

$$\begin{aligned} \mathcal{H}_\Delta &= \Delta \cos 2\theta \sum_{\mathbf{k}} \left(i\sigma_{\alpha\beta}^y \right) \left(c_{1,\mathbf{k}\alpha}^\dagger c_{1,-\mathbf{k}\beta}^\dagger - c_{2,\mathbf{k}\alpha}^\dagger c_{2,-\mathbf{k}\beta}^\dagger \right) + \\ &\Delta \sin 2\theta \sum_{\mathbf{k}} \left(i\sigma_{\alpha\beta}^y \right) \left(c_{1,\mathbf{k}\alpha}^\dagger c_{2,-\mathbf{k}\beta}^\dagger + c_{2,\mathbf{k}\alpha}^\dagger c_{1,-\mathbf{k}\beta}^\dagger \right) + h.c \end{aligned} \quad (5)$$

where σ are Pauli matrices. Note that the inter-band anomalous terms are of the same order Δ as intra-band terms and differ only by their angular dependence. This may seem counterintuitive, as the pairing kernel involving fermions from different bands is much smaller than the kernel involving fermions from the same band. To see why inter-band and intra-band pairing terms are nevertheless comparable, one can explicitly solve for the intra-band and inter-band pairing vertices by using a microscopic interaction that favors d -wave. For concreteness, consider a toy model with pair-hopping interaction:

$$H_{\text{int}} = \frac{g}{2} \sum \left[d_{xz\alpha}^\dagger d_{yz\alpha} d_{xz\beta}^\dagger d_{yz\beta} + d_{yz\alpha}^\dagger d_{xz\alpha} d_{yz\beta}^\dagger d_{xz\beta} \right] \quad (6)$$

$$H_{\text{int}} = -\frac{g}{4} \sum \left[\eta_{1,\mathbf{k}}^\dagger \eta_{1,\mathbf{p}} \cos 2\theta_{\mathbf{k}} \cos 2\theta_{\mathbf{p}} + \eta_{2,\mathbf{k}}^\dagger \eta_{2,\mathbf{p}} \sin 2\theta_{\mathbf{k}} \sin 2\theta_{\mathbf{p}} + (\eta_{1,\mathbf{k}}^\dagger \eta_{2,\mathbf{p}} + \eta_{2,\mathbf{k}}^\dagger \eta_{1,\mathbf{p}}) \sin 2\theta_{\mathbf{p}} \cos 2\theta_{\mathbf{k}} \right] \quad (7)$$

where $\eta_{1,\mathbf{k}}^\dagger = c_{1,\mathbf{k}\alpha}^\dagger c_{1,-\mathbf{k}\beta}^\dagger - c_{2,\mathbf{k}\alpha}^\dagger c_{2,-\mathbf{k}\beta}^\dagger$, $\eta_{2,\mathbf{k}}^\dagger = c_{1,\mathbf{k}\alpha}^\dagger c_{2,-\mathbf{k}\beta}^\dagger + c_{2,\mathbf{k}\alpha}^\dagger c_{1,-\mathbf{k}\beta}^\dagger$, and the summation is over momentum and spin indices. Introducing the two anomalous vertices $\Delta_1 (i\sigma_{\alpha\beta}^y) \eta_{1,\mathbf{k}}^\dagger \cos 2\theta_{\mathbf{k}}$ and $\Delta_2 (i\sigma_{\alpha\beta}^y) \eta_{2,\mathbf{k}}^\dagger \sin 2\theta_{\mathbf{k}}$, and solving the BCS-like gap equations shown graphically in Fig. 3, we obtain

$$\begin{aligned} \Delta_1 &= \frac{g}{4} \left(\frac{\Pi_{11} + \Pi_{22}}{2} \right) \Delta_1 + \frac{g}{4} \Pi_{12} \Delta_2 \\ \Delta_2 &= \frac{g}{4} \Pi_{12} \Delta_2 + \frac{g}{4} \left(\frac{\Pi_{11} + \Pi_{22}}{2} \right) \Delta_1 \end{aligned} \quad (8)$$

where Π_{11}, Π_{22} , and Π_{12} (all positive) are particle-particle polarization bubbles made out of c_1 and c_2 fermions in the superconducting state. Near T_c , we obtain

$$\begin{aligned} \Pi_{11} &= \frac{1}{2} \int d^2\mathbf{k} \frac{\tanh(\frac{\epsilon_{1,\mathbf{k}}}{2T})}{|\epsilon_{1,\mathbf{k}}|}, \quad \Pi_{22} = \frac{1}{2} \int d^2\mathbf{k} \frac{\tanh(\frac{\epsilon_{2,\mathbf{k}}}{2T})}{|\epsilon_{2,\mathbf{k}}|} \\ \Pi_{12} &= \frac{1}{2} \int d^2\mathbf{k} \frac{\tanh(\frac{\epsilon_{1,\mathbf{k}}}{2T}) + \tanh(\frac{\epsilon_{2,\mathbf{k}}}{2T})}{|\epsilon_{1,\mathbf{k}} + \epsilon_{2,\mathbf{k}}|}. \end{aligned} \quad (9)$$

Comparing the two expressions in Eq. (8), we see that $\Delta_1 = \Delta_2 = \Delta$, no matter what is the ratio of the inter-pocket and intra-pocket polarization operators. This holds as long as the interaction g is momentum-independent. If momentum dependence is included, the intra-pocket and inter-pocket interaction terms in (7) differ more than by their distinct angular dependences. In this situation, the r.h.s. of the two equations in (8) are no longer identical, and generally $\Delta_1 > \Delta_2$. In the limiting case $\Delta_2 \rightarrow 0$ one recovers the conventional case with only intra-band pairing condensate.

where the summation over momenta and spin indices is left implicit. A positive g favors B_{1g} pairing as one can verify in a straightforward way by solving the gap equation in the orbital basis. Converting this Hamiltonian into band basis and projecting onto the B_{1g} channel, we obtain

III. EXCITATION SPECTRUM

We now return to Eqs. (3) and (5). The quadratic Hamiltonian $\mathcal{H}_0 + \mathcal{H}_\Delta$ can be straightforwardly diagonalized and yields

$$\mathcal{H} = \sum_{\mathbf{k},\alpha} E_a(\mathbf{k}) a_{\mathbf{k}\alpha}^\dagger a_{\mathbf{k}\alpha} + \sum_{\mathbf{k},\alpha} E_b(\mathbf{k}) b_{\mathbf{k}\alpha}^\dagger b_{\mathbf{k}\alpha} \quad (10)$$

where

$$E_{a,b}(\mathbf{k}) = \sqrt{\Delta^2 \cos^2 2\theta + \epsilon_{a,b}^2(\mathbf{k})} \quad (11)$$

and

$$\begin{aligned} \epsilon_{a,b}(\mathbf{k}) &= \text{sgn}(\epsilon_{1,\mathbf{k}} + \epsilon_{2,\mathbf{k}}) \sqrt{\left(\frac{\epsilon_{1,\mathbf{k}} + \epsilon_{2,\mathbf{k}}}{2} \right)^2 + \Delta^2 \sin^2 2\theta} \\ &\pm \left(\frac{\epsilon_{1,\mathbf{k}} - \epsilon_{2,\mathbf{k}}}{2} \right) \end{aligned} \quad (12)$$

The dispersions $E_{a,b}$ formally have the same forms as in a conventional d -wave superconductor, but are actually more complex because $\epsilon_{a,b}$ themselves depend on Δ . For a vanishing Δ , ϵ_a and ϵ_b coincide with the normal state dispersions, $\epsilon_a = \epsilon_{1,\mathbf{k}}$ and $\epsilon_b = \epsilon_{2,\mathbf{k}}$, as they indeed should. At a finite but small Δ (i.e., near T_c), $\epsilon_a = \epsilon_{1,\mathbf{k}} + \frac{\Delta^2 \sin^2 2\theta}{\epsilon_{1,\mathbf{k}} + \epsilon_{2,\mathbf{k}}}$ and $\epsilon_b = \epsilon_{2,\mathbf{k}} + \frac{\Delta^2 \sin^2 2\theta}{\epsilon_{1,\mathbf{k}} + \epsilon_{2,\mathbf{k}}}$. We see that ϵ_a (ϵ_b) does not vanish on the FS, where $\epsilon_1 = 0$ ($\epsilon_2 = 0$), except along the particular directions $\sin 2\theta = 0$. For such values of θ , however, $\Delta^2 \cos 2\theta$ has a maximum value Δ^2 . As a result, there are no zeroes of $E_{a,b}$ along each of the two FSs, despite the fact that the gap is d -wave. At arbitrary $T < T_c$ we have at $\epsilon_{1,\mathbf{k}} = 0$ (and $\epsilon_{2,\mathbf{k}} > 0$)

$$E_a = \sqrt{\Delta^2 \cos^2 2\theta + \left(\sqrt{\frac{\epsilon_{2,\mathbf{k}}^2}{4} + \Delta^2 \sin^2 2\theta} - \frac{\epsilon_{2,\mathbf{k}}}{2} \right)^2} \quad (13)$$

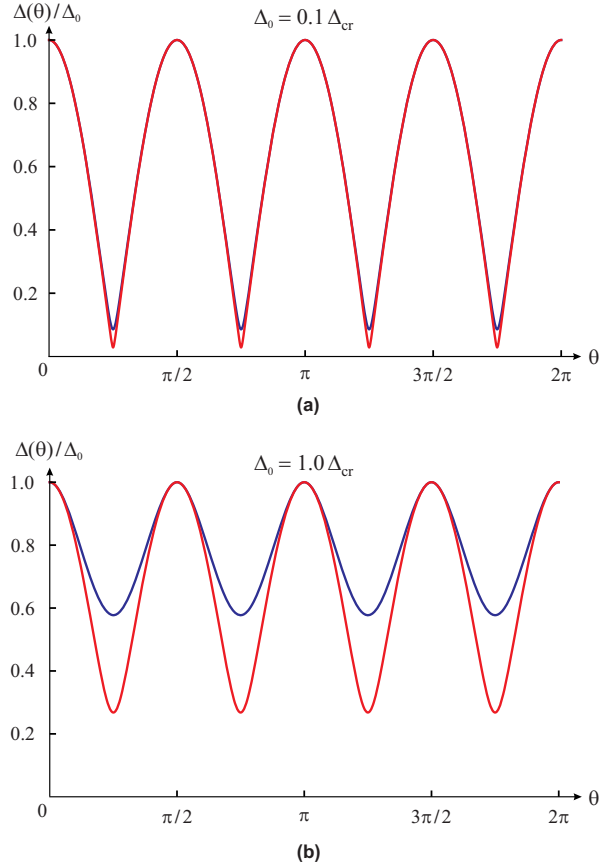


FIG. 4: The dispersion of the d -wave gap along the two FS, Eq. 13, for two values of Δ . Blue (red) lines denote band c_1 (c_2). There is substantial angular variation but no nodes. Note also that the minimum value of the gap is different in both bands.

We plot the excitation energies E_a and E_b as a function of θ along both FS in Fig. 4 for two values of Δ . We see that there is substantial angular variation of $E_{a,b}(\theta)$, but no nodes.

We now analyze the excitation energies $E_{a,b}$ away from the FS. A straightforward analysis of Eq. (12) shows that $\epsilon_{a,b}$ vanish along the lines where

$$\epsilon_{1,\mathbf{k}} \epsilon_{2,\mathbf{k}} = -\Delta^2 \sin^2 2\theta \quad (14)$$

For small Δ (i.e, near T_c), Eq. (14) is satisfied along two separate lines, one adjacent to the inner FS, ($\epsilon_{1,\mathbf{k}} = 0$) and another adjacent to the outer FS ($\epsilon_{2,\mathbf{k}} = 0$). We show the lines $\epsilon_a = 0$ and $\epsilon_b = 0$ in Fig 2 for different values of Δ . Because these lines cross the directions along which $\cos 2\theta = 0$, E_a or E_b vanish at the crossing points, i.e. *the full excitation energy vanishes*. This implies that the nodal points of the d -wave superconductor still exist near T_c , but get shifted away from the normal state FS by the inter-band component of the d -wave gap. The nodal points are located along $\cos 2\theta = 0$, at $k = k_{a,b}$

given by

$$k_{a,b}^2 = \left(\frac{k_{F,1}^2 + k_{F,2}^2}{2} \right) \pm \sqrt{\left(\frac{k_{F,1}^2 - k_{F,2}^2}{2} \right)^2 - 4m_1 m_2 \Delta^2}, \quad (15)$$

where $k_{F,i}^2 = 2m_i \mu$.

The behavior of $E_{a,b}$ at smaller temperatures depends on the interplay between the gap value and the difference between m_2 and m_1 , or specifically, between $\Delta(T)$ and

$$\Delta_{\text{cr}} = \mu \left(\frac{m_2 - m_1}{2\sqrt{m_1 m_2}} \right) \quad (16)$$

If Δ_{cr} is large enough, the nodes survive down to $T = 0$. However, if $m_2 - m_1$ is small enough (i.e., the inner and the outer hole pockets are close), $\Delta(T)$ reaches Δ_{cr} at some $T = T_{\text{cr}}$ below T_c . At this temperature, a Lifshitz transition occurs when the two nodal points merge at $k = k_{\text{cr}}$ and then split in orthogonal directions, see Fig. 2c.

On a technical side, we found that, when Δ is slightly below Δ_{cr} , the two nodal points of the dispersion are the nodes of ϵ_b (and E_b), while the dispersion ϵ_a has no nodes. The change of the behavior from the nodes in both ϵ_a and ϵ_b to two nodes in ϵ_b occurs when Δ reaches the value $\Delta^* = \mu \left(\frac{m_2 - m_1}{m_1 + m_2} \right)$, which is comparable but smaller than Δ_{cr} . The ratio $\Delta^*/\Delta_{\text{cr}} = 2\sqrt{m_1 m_2}/(m_1 + m_2) < 1$. This change does not affect the location of the zeros of $\epsilon_{a,b}$ in momentum space (gray lines in Fig. Fig. 2), just the identification of these lines with ϵ_a or ϵ_b becomes more complex.

At $\Delta > \Delta_{\text{cr}}$, the lines where $\epsilon_{a,b} = 0$ form four disconnected closed loops (see Fig. 2d). Along these loops the excitation energy becomes $E = \Delta |\cos 2\theta|$. However, because the closed loops do not cross the directions $\cos 2\theta = 0$, the nodes disappear, i.e. the excitation spectrum of a d -wave superconductor becomes *fully gapped*.

IV. ANALOGY WITH SEMI-METAL TO INSULATOR TRANSITION

There is a close analogy between the Lifshitz transition at $T = T_{\text{cr}}$ in our problem and the transition from a 2D massless Dirac semi-metal to an insulator. In the latter case, the semi-metal phase has two separate Dirac nodal points with the winding numbers ± 1 ¹⁷. Upon variation of some system parameter (e.g., strain in graphene), the distance between the two nodal points decreases until they merge and annihilate at a critical value of such parameter. At the critical point, the system is described by fermions with linear dispersion in one spatial direction and quadratic in the other.¹⁸⁻²⁰ Similarly, in our case, near T_c , the dispersion along one of the four directions specified by $\cos 2\theta = 0$ has two nodal points with Dirac-like dispersions. Just as in the semi-metal to insulator transition, the winding numbers near the

two Dirac points are ± 1 . At $T = T_{\text{cr}}$ (if it exists), the Dirac points merge. At this temperature the excitation spectrum around the single nodal point is quadratic along the direction in which $\cos 2\theta = 0$ and linear in the transverse direction. At a smaller temperature, the excitation spectrum is fully gapped, like in an insulator. Recent studies of the semi-metal to insulator transition have shown¹⁹ that at the critical point the dynamically screened Coulomb interaction gives rise to a highly non-trivial quantum-critical behavior in both fermionic and bosonic sectors. A d -wave state in the FeSC will provide a realization of such behavior if T_{cr} can be tuned to zero by changing some external parameter, such as pressure.

A somewhat different Lifshitz transition can also take place in an s^{+-} -wave state of a FeSC, if accidental nodes merge and disappear under a change of system parameters^{24–27}, such as application of strain²⁸.

V. CONCLUSIONS

In this work we analyzed the d -wave gap structure of multi-orbital FeSC, as several experimental and theoretical studies suggested that such a state may be realized in materials with only hole-like or only electron-like Fermi pockets. We showed that the common belief that a d -wave gap must have nodes on a closed Fermi surface located at the center of the Brillouin zone is correct only if this Fermi surface is made out of a single orbital, but it is not necessarily true if there is an even number of pockets made out of different orbitals.

In particular, for the Γ -centered hole pockets present in most FeSC, which are made out of d_{xz} and d_{yz} orbitals, there are no d -wave gap nodes in either Fermi surface. Depending on the magnitude of the gap, as compared to the relative radii of the two Fermi surfaces, the $d_{x^2-y^2}$ -wave nodal points are either displaced from the Fermi surface along the diagonal direction, or are com-

pletely absent. A Lifshitz transition, in which the Dirac gap nodes annihilate, is analogous to a transition from a 2D massless Dirac semi-metal to an insulator. Because the electron pockets are small and centered at $(\pi, 0)$ and $(0, \pi)$, they do not cross the diagonals of the Brillouin zone, i.e. there are no d -wave gap nodes on these pockets as well. Thus, a d -wave FeSC with two d_{xz}/d_{yz} hole pockets and two electron pockets may display a completely nodeless d -wave superconductivity.

Our results have important consequences for the experimental identification of d -wave states in FeSC. In particular, the fact that ARPES does not see nodes in the d_{xz}/d_{yz} Fermi surface of KFe_2As_2 is, in principle, not inconsistent with a d -wave state. However, based on the values of the gap and of the radii of the d_{xz}/d_{yz} hole pockets extracted from ARPES, it is likely that the nodes are still present, but away from the FS. In this regard, only precise measurements of the gap along the hole pockets made predominantly out of a single orbital can qualitatively distinguish between nodal s^{+-} and d -wave states. In this regard, the observation of a nodeless gap in $\text{K}_x\text{Fe}_{2-y}\text{Se}_2$ on a Z -pocket consisting of a single orbital, provides strong evidence against a d -wave state.

VI. ACKNOWLEDGEMENTS

We are thankful to E. Berg, S. Borisenko, P. Coleman, L. Fu, P. Hirschfeld, Y. Matsuda, J. Schmalian, and Q. Si for useful discussions. This work was supported by the Office of Basic Energy Sciences, U.S. Department of Energy, under awards DE-SC0014402 (AVC) and DE-SC0012336 (RMF). O.V. was supported by NSF grant DMR 1506756. The authors thank the hospitality of the Aspen Center for Physics, where part of this work was performed. ASP is supported by NSF grant PHY-1066293.

¹ For recent reviews see J-P Paglione and R.L. Greene, *Nature Phys.* **6**, 645 (2010), I.I. Mazin, *Nature* **464**, 183 (2010), H.H. Wen and S. Li, *Annu. Rev. Condens. Matter Phys.*, **2**, 121 (2011), D.N. Basov and A.V. Chubukov, *Nature Physics* **7**, 241 (2011), P.J. Hirschfeld, M.M. Korshunov, and I.I. Mazin, *Rev. Prog. Phys.* **74**, 124508 (2011), A.V. Chubukov, *Annual Review of Condensed Matter Physics* **3**, 57 (2012); R. M. Fernandes, A. V. Chubukov, and J. Schmalian, *Nature Phys.* **10**, 97 (2014).

² I. I. Mazin, D. J. Singh, M. D. Johannes, and M. H. Du, *Phys. Rev. Lett.* **101**, 057003 (2008); K. Kuroki, S. Onari, R. Arita, H. Usui, Y. Tanaka, H. Kontani, and H. Aoki *Phys. Rev. Lett.* **101**, 087004 (2008); A. V. Chubukov, D. Efremov, and I. Eremin, *Phys. Rev. B* **78**, 134512 (2008).

³ T. Yoshida, I. Nishi, A. Fujimori, M. Yi, R. G. Moore, D. Lu, Z. Shen, K. Kihou, P. M. Shirage, H. Kito, C. H. Lee, A. Iyo, H. Eisaki, and H. Harima, arXiv:1007.2698; K. Hashimoto, A. Serafin, S. Tonegawa, R. Katsumata,

R. Okazaki, T. Saito, H. Fukazawa, Y. Kohori, K. Kihou, C. H. Lee, A. Iyo, H. Eisaki, H. Ikeda, Y. Matsuda, A. Carrington, T. Shibauchi, *Phys. Rev. B* **82**, 014526 (2010); T. Terashima et al., *J. Phys. Soc. Jpn.* **79**, 053702 (2010); Hardy, F. et al. *Phys. Rev. Lett.* **111**, 027002 (2013).

⁴ T. Sato, K. Nakayama, Y. Sekiba, P. Richard, Y.-M. Xu et al., *Phys. Rev. Lett.* **103**, 047002 (2009); V. B. Zabolotnyy, D. V. Evtushinsky, A. A. Kordyuk, D. S. Inosov, A. Koitzsch, A. V. Boris, G. L. Sun, C. T. Lin, M. Knupfer, B. Buechner, A. Varykhalov, R. Follath, S. V. Borisenko, *Physica C* **469**, 448-451 (2009); D. V. Evtushinsky, T. K. Kim, A. A. Kordyuk, V. B. Zabolotnyy, B. Büchner, A. V. Boris, D. L. Sun, C. T. Lin, H. Q. Luo, Z. S. Wang, H. H. Wen, R. Follath, and S. V. Borisenko, arXiv:1106.4584. The electronic structure with 3 hole pockets at Γ point and hole blades at the corners of the 2Fe Brillouin zone is consistent with DFT band structure calculations for this material [see e.g., T. Terashima, M. Kimata, N. Kurita,

H. Satsukawa, A. Harada, K. Hazama, M. Imai, A. Sato, K. Kihou, C.-H. Lee, H. Kito, H. Eisaki, A. Iyo, T. Saito, H. Fukazawa, Y. Kohori, H. Harima, and S. Uji, *J. Phys. Soc. Jpn.* **79**, 053702 (2010)].

⁵ J. Guo, S. Jin, G. Wang, S. Wang, K. Zhu, T. Zhou, M. He, and X. Chen, *Phys. Rev. B* **82**, 180520(R) (2010). See Y. Liu, Z. C. Li, W. P. Liu, G. Friemel, D. S. Inosov, R. E. Dinnebier, Z. J. Li, and C. T. Lin, *Supercond. Sci. Technol.* **25**, 075001 (2012); T. Qian, X.-P. Wang, W.-C. Jin, P. Zhang, P. Richard, G. Xu, X. Dai, Z. Fang, J.-G. Guo, X.-L. Chen, H. Ding, *Phys. Rev. Lett.* **106**, 187001 (2011).

⁶ J. K. Dong, S. Y. Zhou, T. Y. Guan, H. Zhang, Y. F. Dai, X. Qiu, X. F. Wang, Y. He, X. H. Chen, and S. Y. Li, *Phys. Rev. Lett.* **104**, 087005 (2010); J.-Ph. Reid, M. A. Tanatar, A. Juneau-Fecteau, R. T. Gordon, S. Rene de Cotret, N. Doiron-Leyraud, T. Saito, H. Fukazawa, Y. Kohori, K. Kihou, C. H. Lee, A. Iyo, H. Eisaki, R. Prozorov, and L. Taillefer, *Phys. Rev. Lett.* **109**, 087001 (2012). For alternative explanation of thermal conductivity see D. Watanabe, T. Yamashita, Y. Kawamoto, S. Kurata, Y. Mizukami, T. Ohta, S. Kasahara, M. Yamashita, T. Saito, H. Fukazawa, Y. Kohori, S. Ishida, K. Kihou, C. H. Lee, A. Iyo, H. Eisaki, A. B. Vorontsov, T. Shibauchi, and Y. Matsuda, *Phys. Rev. B* **89**, 115112 (2014); F. F. Tafti, A. Juneau-Fecteau, M.-È. Delage, S. René de Cotret, J.-Ph. Reid, A. F. Wang, X.-G. Luo, X. H. Chen, N. Doiron-Leyraud, and L. Taillefer, *Nature Phys.* **9**, 349 (2013). For the behavior of thermal conductivity under pressure see F. F. Tafti, J. P. Clancy, M. Lapointe-Major, C. Collignon, S. Faucher, J. Sears, A. Juneau-Fecteau, N. Doiron-Leyraud, A. F. Wang, X. G. Luo, X. H. Chen, S. Desgreniers, Young-June Kim, and Louis Taillefer, *Phys. Rev. B* **89**, 134502 (2014).

⁷ T. Böhm, A.F. Kemper, B. Moritz, F. Kretzschmar, B. Muschler, H.-M. Eiter, R. Hackl, T. P. Devereaux, D. J. Scalapino, and Hai-Hu Wen, *Phys. Rev. X* **4**, 041046 (2014). For an alternative explanation see M. Khodas, A. V. Chubukov, and G. Blumberg *Phys. Rev. B* **89**, 245134 (2014).

⁸ G. Friemel et al, *Phys. Rev. B* **85**, 140511 (2012).

⁹ L. Zhao, D. Mou, S. Liu, X. Jia, J. He, et al., *Phys. Rev. B* **83**, 140508 (2011); M. Xu, Q. Q. Ge, R. Peng, Z. R. Ye, J. Jiang, et al., *Phys. Rev. B* **85**, 220504 (2012).

¹⁰ T. A. Maier, S. Graser, P. J. Hirschfeld, and D. J. Scalapino, *Phys. Rev. B* **83**, 100515 (2011); A. Kreisel, Y. Wang, T. A. Maier, P. J. Hirschfeld, D. J. Scalapino, *Phys. Rev. B* **88**, 094522 (2013); T. Das and A. V. Balatsky, *Phys. Rev. B* **84**, 014521 (2011), *Phys. Rev. B* **84**, 115117 (2011); F. Wang, F. Yang, M. Gao, Z.-Y. Lu, T. Xiang *et al*, *Europhys. Lett.*, **93**, 57003 (2011); Fa Wang, Fan Yang, Miao Gao, Zhong-Yi Lu, Tao Xiang, and Dung-Hai Lee, *Europhy. Lett.* **93**, 57003 (2011); Fan Yang, Fa Wang, and Dung-Hai Lee *Phys. Rev. B* **88**, 100504 (2013); R. M. Fernandes and A. J. Millis, *Phys. Rev. Lett.* **110**, 117004 (2013). For an alternative proposal for sign-changing s^+ -gap between hybridized hole pockets see I. I. Mazin, *Phys. Rev. B* **84**, 024529 (2011); M. Khodas and A. V. Chubukov *Phys. Rev. Lett.* **108**, 247003 (2012), *Phys. Rev. B* **86**, 144519 (2012).

¹¹ R. Thomale, C. Platt, W. Hanke, J. Hu, and B. A. Bernevig, *Phys. Rev. Lett.* **107**, 117001 (2011).

¹² S. Maiti, M.M. Korshunov, T.A. Maier, P.J. Hirschfeld, A.V. Chubukov, *Phys. Rev. Lett.* **107**, 147002 (2011); *Phys. Rev. B* **84**, 224505 (2011); K. Suzuki, H. Usui, and K. Kuroki, *arXiv:1108.0657v1* (2011).

¹³ K. Okazaki, Y. Ota, Y. Kotani, W. Malaeb, Y. Ishida, T. Shimojima, T. Kiss, S. Watanabe, C.-T. Chen, K. Kihou, C. H. Lee, A. Iyo, H. Eisaki, T. Saito, H. Fukazawa, Y. Kohori, K. Hashimoto, T. Shibauchi, Y. Matsuda, H. Ikeda, H. Miyahara, R. Arita, A. Chainani, S. Shin, *Science* **337**, 1314 (2012).

¹⁴ The superconducting gap on this pocket is visible in the data, and its angular variation can be inferred without additional analysis.

¹⁵ Z. P. Yin, K. Haule, and G. Kotliar, *Nature Phys.* **10**, 845 (2014); J. Hu, *Phys. Rev. X* **3**, 031004 (2013); T. Ong, P. Coleman, and J. Schmalian, *PNAS* **113**, 5486 (2016).

¹⁶ A. V. Chubukov, M. Khodas, and R. M. Fernandes, *arXiv:1602.05503*.

¹⁷ In graphene Dirac nodal points with winding number ± 1 are located at the $\pm K$ points of the honeycomb lattice, see O. Vafek and A. Vishwanath, *Annu. Rev. Condens. Matter Phys.*, **5**, 83 (2014).

¹⁸ G. Montambaux, F. Piechon, J.-N. Fuchs, and M. O. Goerbig, *Eur. Phys. J. B* **72**, 509 (2009); G. Montambaux, F. Piechon, J.-N. Fuchs, and M. O. Goerbig, *Phys. Rev. B* **80**, 153412 (2009).

¹⁹ H. Isobe, Bohm-Jung Yang, A.V. Chubukov, J. Schmalian, and N. Nagaosa, *Phys. Rev. Lett.* **116**, 076803 (2016).

²⁰ G-Y. Cho and E-G Moon, *Scientific Reports*, **6**, 19198 (2016).

²¹ Q. Si, private communication.

²² V. Cvetkovic and O. Vafek, *Phys. Rev. B* **88**, 134510 (2013).

²³ R. M. Fernandes and O. Vafek, *Phys. Rev. B* **90**, 214514 (2014).

²⁴ R. M. Fernandes and J. Schmalian, *Phys. Rev. B* **84**, 012505 (2011).

²⁵ V. Stanev, B. S. Alexandrov, P. Nikolic, and Z. Tesanovic, *Phys. Rev. B* **84**, 014505 (2011).

²⁶ B. Mazidian, J. Quintanilla, A. D. Hillier, and J. F. Annett, *Phys. Rev. B* **88**, 224504 (2013).

²⁷ M. Khodas and A. V. Chubukov, *Phys. Rev. B* **86**, 144519 (2012); A. Hinojosa and A.V. Chubukov, *Phys. Rev. B* **91**, 224502 (2015).

²⁸ J. Kang, A.F. Kemper, and R. M. Fernandes *Phys. Rev. Lett.* **113**, 217001 (2014).